



HAL
open science

Pharmacodynamic, pharmacokinetic and rat brain receptor occupancy profile of NLX-112, a highly selective 5-HT 1A receptor biased agonist

Ronan Y Depoortère, Andrew C McCreary, Benjamin Vidal, Mark A Varney,
Luc Zimmer, Adrian Newman-Tancredi

► To cite this version:

Ronan Y Depoortère, Andrew C McCreary, Benjamin Vidal, Mark A Varney, Luc Zimmer, et al.. Pharmacodynamic, pharmacokinetic and rat brain receptor occupancy profile of NLX-112, a highly selective 5-HT 1A receptor biased agonist. *Naunyn-Schmiedeberg's Archives of Pharmacology*, 2024, 398 (1), pp.991-1002. 10.1007/s00210-024-03323-0 . hal-04932477

HAL Id: hal-04932477

<https://hal.science/hal-04932477v1>

Submitted on 6 Feb 2025

HAL is a multi-disciplinary open access archive for the deposit and dissemination of scientific research documents, whether they are published or not. The documents may come from teaching and research institutions in France or abroad, or from public or private research centers.

L'archive ouverte pluridisciplinaire **HAL**, est destinée au dépôt et à la diffusion de documents scientifiques de niveau recherche, publiés ou non, émanant des établissements d'enseignement et de recherche français ou étrangers, des laboratoires publics ou privés.

Metadata of the article that will be visualized in OnlineFirst

ArticleTitle	Pharmacodynamic, pharmacokinetic and rat brain receptor occupancy profile of NLX-112, a highly selective 5-HT _{1A} receptor biased agonist	
--------------	-----------------------------------------------------------------------------------------------------------------------------------------------------	--

Article Sub-Title		
-------------------	--	--

Article CopyRight	The Author(s), under exclusive licence to Springer-Verlag GmbH Germany, part of Springer Nature (This will be the copyright line in the final PDF)	
-------------------	----------------------------------------------------------------------------------------------------------------------------------------------------	--

Journal Name	Naunyn-Schmiedeberg's Archives of Pharmacology	
--------------	------------------------------------------------	--

Corresponding Author	FamilyName	Newman-Tancredi
	Particle	
	Given Name	Adrian
	Suffix	
	Division	
	Organization	Neurolix SAS
	Address	2 Rue Georges Charpak, 81100, Castres, France
	Phone	
	Fax	
	Email	anewmantancredi@neurolix.com
	URL	
ORCID		

Author	FamilyName	Depoortère
	Particle	
	Given Name	Ronan Y.
	Suffix	
	Division	
	Organization	Neurolix SAS
	Address	2 Rue Georges Charpak, 81100, Castres, France
	Phone	
	Fax	
	Email	
	URL	
ORCID		

Author	FamilyName	McCreary
	Particle	
	Given Name	Andrew C.
	Suffix	
	Division	
	Organization	Brains On-Line
	Address	Groningen, Netherlands
	Division	
	Organization	GW Pharmaceuticals
	Address	Cambridge, UK
	Phone	
Fax		
Email		
URL		
ORCID		

Author	FamilyName	Vidal
--------	------------	--------------

Particle
Given Name **Benjamin**
Suffix
Division
Organization Université Claude Bernard Lyon 1, Lyon Neuroscience Research Center,
CNRS, INSERM, CERMEP-Imaging Platform
Address Bron, France
Phone
Fax
Email
URL
ORCID

Author FamilyName **Varney**
Particle
Given Name **Mark A.**
Suffix
Division
Organization Neurolix SAS
Address 2 Rue Georges Charpak, 81100, Castres, France
Phone
Fax
Email
URL
ORCID

Author FamilyName **Zimmer**
Particle
Given Name **Luc**
Suffix
Division
Organization Université Claude Bernard Lyon 1, Lyon Neuroscience Research Center,
CNRS, INSERM, CERMEP-Imaging Platform
Address Bron, France
Division
Organization Hospices Civils de Lyon
Address Lyon, France
Phone
Fax
Email
URL
ORCID

Schedule Received 20 Mar 2024
Revised
Accepted 22 Jul 2024

Abstract NLX-112 (i.e., F13640, befiradol) exhibits nanomolar affinity, exceptional selectivity and full agonist efficacy at serotonin 5-HT_{1A} receptors. NLX-112 shows efficacy in rat, marmoset and macaque models of L-DOPA induced dyskinesia (LID) in Parkinson's disease and has shown clinical efficacy in a Phase 2a proof-of-concept study for this indication. Here we investigated, in rats, its pharmacodynamic, pharmacokinetic (PK) and brain 5-HT_{1A} receptor occupancy profiles, and its PK properties in the absence and presence of L-DOPA. Total and free NLX-112 exposure in plasma, CSF and striatal ECF was dose-proportional over the range tested (0.04, 0.16 and 0.63 mg/kg i.p.). NLX-112 exposure increased rapidly (T_{max} 0.25–0.5h) and exhibited approximately threefold longer half-life in brain than in plasma (1.1 and 3.6h, respectively). At a pharmacologically relevant dose of 0.16 mg/kg i.p., previously shown to elicit anti-LID activity in parkinsonian rats, brain concentration of NLX-112 was 51–63 ng/g from 0.15 to 1h. In microPET imaging experiments, NLX-112 showed dose-dependent reduction of 18F-F13640 (i.e., 18F-NLX-112) brain 5-HT_{1A} receptor labeling in cingulate cortex and

striatum, regions associated with motor control and mood, with almost complete inhibition of labeling at the dose of 0.63 mg/kg i.p.. Co-administration of L-DOPA (6 mg/kg s.c., a dose used to elicit LID in parkinsonian rats) together with NLX-112 (0.16 mg/kg i.p.) did not modify PK parameters in rat plasma and brain of either NLX-112 or L-DOPA. Here, we demonstrate that NLX-112's profile is compatible with 'druggable' parameters for CNS indications, and of the results provide measures of brain concentrations and 5-HT_{1A} receptor binding parameters relevant to the anti-dyskinetic activity of the compound.

Keywords (separated by '-') 5-HT_{1A} receptors - Dyskinesia - NLX-112 - L-DOPA - Parkinson's disease - Pharmacokinetics - Rat

Footnote Information The online version contains supplementary material available at <https://doi.org/10.1007/s00210-024-03323-0> .



2 Pharmacodynamic, pharmacokinetic and rat brain receptor occupancy 3 profile of NLX-112, a highly selective 5-HT_{1A} receptor biased agonist

4 Ronan Y. Depoortère¹ · Andrew C. McCreary^{2,3} · Benjamin Vidal⁴ · Mark A. Varney¹ · Luc Zimmer^{4,5} ·
5 Adrian Newman-Tancredi¹

6 Received: 20 March 2024 / Accepted: 22 July 2024

7 © The Author(s), under exclusive licence to Springer-Verlag GmbH Germany, part of Springer Nature 2024

AQ1 Abstract

AQ2 NLX-112 (i.e., F13640, befiradol) exhibits nanomolar affinity, exceptional selectivity and full agonist efficacy at serotonin
AQ3 5-HT_{1A} receptors. NLX-112 shows efficacy in rat, marmoset and macaque models of L-DOPA induced dyskinesia (LID)
11 in Parkinson's disease and has shown clinical efficacy in a Phase 2a proof-of-concept study for this indication. Here we
12 investigated, in rats, its pharmacodynamic, pharmacokinetic (PK) and brain 5-HT_{1A} receptor occupancy profiles, and its
13 PK properties in the absence and presence of L-DOPA. Total and free NLX-112 exposure in plasma, CSF and striatal ECF
14 was dose-proportional over the range tested (0.04, 0.16 and 0.63 mg/kg i.p.). NLX-112 exposure increased rapidly (T_{max}
15 0.25–0.5h) and exhibited approximately threefold longer half-life in brain than in plasma (1.1 and 3.6h, respectively). At a
16 pharmacologically relevant dose of 0.16 mg/kg i.p., previously shown to elicit anti-LID activity in parkinsonian rats, brain
17 concentration of NLX-112 was 51–63 ng/g from 0.15 to 1h. In microPET imaging experiments, NLX-112 showed dose-
18 dependent reduction of ¹⁸F-F13640 (i.e., ¹⁸F-NLX-112) brain 5-HT_{1A} receptor labeling in cingulate cortex and striatum,
19 regions associated with motor control and mood, with almost complete inhibition of labeling at the dose of 0.63 mg/kg i.p..
20 Co-administration of L-DOPA (6 mg/kg s.c., a dose used to elicit LID in parkinsonian rats) together with NLX-112 (0.16 mg/
21 kg i.p.) did not modify PK parameters in rat plasma and brain of either NLX-112 or L-DOPA. Here, we demonstrate that
22 NLX-112's profile is compatible with 'druggable' parameters for CNS indications, and of the results provide measures of
23 brain concentrations and 5-HT_{1A} receptor binding parameters relevant to the anti-dyskinetic activity of the compound.

24 **Keywords** 5-HT_{1A} receptors · Dyskinesia · NLX-112 · L-DOPA · Parkinson's disease · Pharmacokinetics · Rat

25 Introduction

26 Serotonin (5-hydroxytryptamine, 5-HT) 1A (5-HT_{1A}) recep-
27 tors are important targets for treatment of a variety of indica-
28 tions, e.g. depression and anxiety, acute and chronic pain,
29 and movement disorders (Borroto-Escuela et al. 2021;

Pagano et al. 2017; Celada et al. 2013; Barnes et al. 2021; 30
Pourhamzeh et al. 2021). In movement disorders, such as 31
Parkinson's disease (PD), activation of these receptors is 32
associated with alleviation of motor dysfunctions in both 33
animal models and human pathological states; for example, 34
5-HT_{1A} receptor agonists such as 8-OH-DPAT, buspirone 35
and ipsapirone attenuate haloperidol-induced catalepsy, a 36
rat model of parkinsonian rigidity (Prinssen et al. 2002). 37
In clinical trials, the early 5-HT_{1A} receptor agonists, bus- 38
pirone and sarizotan reduced dyskinesia in PD patients, 39
who had received protracted treatment with L-DOPA (Levo 40
3,4-dihydroxyphénylalanine, the gold standard treatment 41
for parkinsonism), but, unfortunately, also interfered with 42
the anti-parkinsonian effects of the latter. This interference 43
is likely due to the fact that these compounds also display 44
antagonist activity at dopamine D₂ receptors, thus facili- 45
tating parkinsonism. Compounds such as buspirone also 46
lack substantial agonist efficacy (they are partial agonists 47

A1 ✉ Adrian Newman-Tancredi
A2 anewmantancredi@neurolixis.com

A3 ¹ Neurolixis SAS, 2 Rue Georges Charpak, 81100 Castres,
A4 France

A5 ² Brains On-Line, Groningen, Netherlands

A6 ³ Present Address: GW Pharmaceuticals, Cambridge, UK

A7 ⁴ Université Claude Bernard Lyon 1, Lyon Neuroscience
A8 Research Center, CNRS, INSERM, CERMEP-Imaging
A9 Platform, Bron, France

A10 ⁵ Hospices Civils de Lyon, Lyon, France

at 5-HT_{1A} receptors), and are rapidly degraded to the active metabolite 1-(2-pyrimidinyl)piperazine (1-PP) (Caccia et al. 1983; Newman-Tancredi et al. 2022).

Unlike older agonists, NLX-112 (a.k.a. F13640 or befiradol), shows a promising profile: it is exceptionally selective for and displays full agonist efficacy at 5-HT_{1A} receptors (Newman-Tancredi et al. 2017), notably in brain regions associated with motor coordination (Vidal et al. 2020; Levigoureux et al. 2019; Newman-Tancredi et al. 2022). Moreover, NLX-112 is robustly active in animal models of abnormal motor behaviors. Hence, in rats rendered hemiparkinsonian by 6-OHDA lesioning of the nigrostriatal dopaminergic pathway, chronic treatment with L-DOPA produces abnormal involuntary movements (AIMs), considered to mimic L-DOPA-induced dyskinesia (LID) in PD patients. NLX-112 (0.01 to 0.16 mg/kg i.p.) potently and efficaciously reduced AIMs scores (Iderberg et al. 2015). Similarly, in non-human primates (marmosets and cynomolgus macaques) rendered parkinsonian-like by administration of the neurotoxin MPTP, and rendered dyskinetic with protracted treatment with L-DOPA, NLX-112 dose-dependently attenuated LID (Depoortere et al. 2020), (Fisher et al. 2020) (see Supplementary file for more in-depth description of LID, and the rationale for using NLX-112 to attenuate it). NLX-112 is currently under clinical development for treatment of LID in PD patients and successfully completed a proof-of-concept Phase 2a trial (ClinicalTrials.gov ID #NCT05148884) in which it met both its primary outcome of safety and tolerability, its secondary outcome of efficacy against LID and also diminished parkinsonian motor disability (Svenningsson et al. 2023).

Despite the fact that NLX-112 has been extensively investigated for its pharmacodynamic activity in a variety of animal models (see recent review by (Newman-Tancredi et al. 2022) for extended details), the relationship between its pharmacodynamic and its pharmacokinetic (PK) profiles has received limited attention. Hence, Bardin and collaborators (Bardin et al. 2005) reported data for total plasma exposure of NLX-112 (0.01 to 2.5 mg/kg i.p.), together with exposure measured from hippocampal microdialysate samples and compared it to behavioral effects in models of pain. However, they did not report free plasma exposure or, importantly, the levels of NLX-112 in the striatum, a brain structure involved in motor control and relevant to the development of NLX-112 for movement disorders.

The present study therefore investigated additional pharmacokinetic characteristics of NLX-112 after i.p. administration at pharmacologically active doses in male rats. Firstly, we explored the exposure levels of NLX-112 in plasma (total and free levels), in cerebrospinal fluid (total CSF levels) and in the striatum (free extra cellular fluid: ECF). Secondly, we undertook a microPET imaging study in which we explored the ability of unlabeled NLX-112

(administered i.p.) to displace binding of ¹⁸F-F13640 (i.e., ¹⁸F-labeled NLX-112), as a brain penetrant radiotracer to selectively label 5-HT_{1A} receptors (Colom et al. 2021, 2020; Vidal et al. 2014, 2018). The goal was to estimate the level of 5-HT_{1A} receptor occupancy at doses that produce anti-LID activity. Thirdly, we showed that co-administration of NLX-112 and L-DOPA did not alter the PK profiles of either of the compounds, supporting the conclusion that their effects are mediated independently of PK interactions. Overall, the present PK/PD and brain imaging study provides important exposure and target engagement information supporting the development of NLX-112 for LID.

Methods

Animals for drug exposure determinations

Total plasma, free blood (measured with ultraslow microdialysis, see below), total CSF and free striatal ECF exposure were determined in adult male Sprague–Dawley rats (weight 314–372 g, approximately 8 weeks old upon arrival in the laboratory, Harlan, the Netherlands), housed in polypropylene cages (40 X 50 X 20 cm³) with wire mesh tops, in groups of 5 animals per cage. All animals had ad libitum access to standard rat chow (RMH-B 2181, HopeFarms BV, Woerden, NL) and tap water. Animals were housed in temperature (22 ± 2 °C) and humidity (55 ± 10%) controlled environment, using a 12-h light–dark cycle (lights on 07.00 – 19.00). Environmental enrichment was made available to all animals. All experiments were conducted in strict accordance with the National Institutes of Health “*Care and Use of Laboratory Animals*” guidelines, and with the Dutch law, and were approved by the Animal Care and Use Committee of the University of Groningen, the Netherlands.

A separate NLX-112/L-DOPA plasma and brain exposure study (alone and in combination) was carried out using adult male Sprague–Dawley rats (SLAC Laboratory Animal Co. Ltd., Shanghai, China). Animals were group-housed and acclimated for at least 3 days before being used. The animal room environment was controlled (20 to 26 °C, humidity 30 to 70%), 12 h artificial light and 12 h dark). Animals had ad libitum access to tap water and to Certified Rodent Diet (Beijing KEAO XIELI Feed Co., Ltd. Beijing, China) 4 h post dosing.

Surgery for implantation of striatal microdialysis probes

Before surgery, Fynadine[®] (1 mg/kg s.c.) was administered to provide peri- and post-operative analgesia. Rats were anesthetized using isoflurane (2% and 500 mL/min O₂), the anesthesia was maintained throughout the duration of

AQ4 3

148 surgery. A mixture of excess topically applied bupivacaine
149 (5 mg/mL) and epinephrine (5 µg/mL) was used for local
150 anesthesia of the surgical sites. Rats were positioned into a
151 stereotaxic apparatus (David Kopf Instruments, Tujunga, CA
152 91042, USA) for implantation with a MetaQuant ultraslow
153 flow microdialysis probe (4 mm exposed microdialysate poly-
154 acrylonitrile membrane; Brainlink, Groningen, the Nether-
155 lands) in the striatum (coordinates: anterior +0.6 mm from
156 Bregma, lateral from midline -3.5 mm, ventral -7.5 mm from
157 dura and the incisor-bar set to -3.3 mm for flat-skull position
158 (Paxinos and Watson 2007).

159 **Surgery for cannulation of jugular and femoral** 160 **veins and Cisterna Magna**

161 Using a surgical procedure identical to that described above,
162 a 10 cm segment of silicone tubing (0.64 mm ID; 0.94 mm
163 OD, Brainlink, Groningen, the Netherlands) was inserted
164 4.2 mm deep from the point of venous insertion for the
165 jugular vein and 2 mm deep for the femoral vein. Catheter
166 patency was maintained by filling with 88% glycerol solu-
167 tion containing 500 IE/mL heparin.

168 For the Cisterna Magna, a cannula equipped with a
169 dummy cannula, was inserted at the level of the occipital
170 parietal junction (coordinates: on midline (0 mm), ventral
171 -4.5 to 5.5 mm from the dura, with the incisor-bar set to
172 3.3 mm). When the cannula was inserted, tell-tale CSF flow
173 was witnessed by the brief removal of the dummy cannula.
174 Catheters, microdialysis probes and Cisterna Magna cannu-
175 lae, were exteriorized following subcutaneous tunneling and
176 affixed to the skull with dental cement and stainless-steel
177 screws for additional stability.

178 In animals receiving a femoral vein catheter, an ultra-
179 slow flow microdialysis probe (MQ-JV-RC 800/040, with
180 a 4.2 mm indwelling cannula; Brainlink, Groningen, the
181 Netherlands) was also inserted into the jugular vein for the
182 measurement of free plasma levels of NLX-112.

183 **Total and free plasma, total CSF and free striatum** 184 **NLX-112 exposure by ultraslow microdialysis**

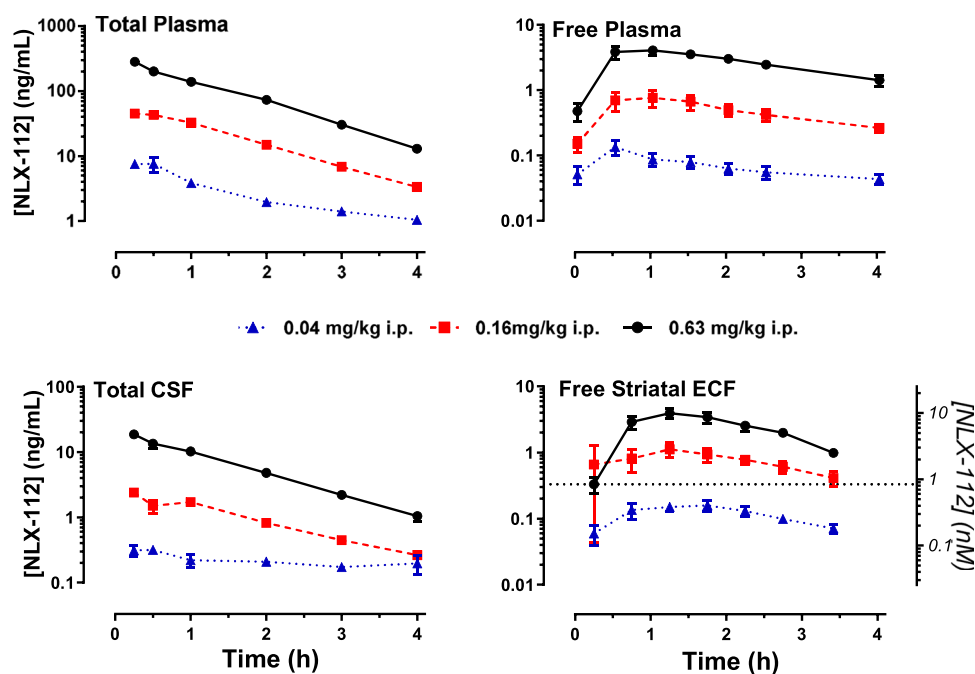
185 All studies were conducted in awake, freely moving rats.
186 For determination of total levels of NLX-112 in plasma the
187 following procedure was followed. Sample preparation was
188 carried out by mixing 5 µL of plasma sample with a 45 µL
189 of a precipitation solution (16 mL acetonitrile, 3.78 mL
190 ultrapurified water, 200 µL 1% ascorbic acid, 20 µL formic
191 acid). This was vortexed for 10 s and after 5 min at room
192 temperature was centrifuged at 13,000 rpm for 5 min at 4° C
193 and 10 µL of the supernatant was added to 90 µL of a blank
194 matrix (19.78 mL UP H₂O, 20 µL formic acid and 200 µL
195 1% ascorbic acid).

196 For determination of free plasma, free striatum and total
197 CSF levels of NLX-112, the following procedure was fol-
198 lowed. Following microdialysis probe and cannula implan-
199 tation and overnight recovery from surgery, the probes
200 were connected to a microperfusion pump (Syringe pump,
201 CMA, Sweden) and perfused with artificial CSF (147 mM
202 NaCl, 3.0 mM KCl, 1.2 mM CaCl₂, and 1.2 mM MgCl₂,
203 without 0.2% BSA). The flow rate was 0.12 µL/min with a
204 carrier flow of 0.80 µL/min. After 60 min of pre-stabiliza-
205 tion, microdialysis samples were collected at various time
206 points between 0.25 and 4 h after drug administration (see
207 Fig. 1). Samples were collected in tared mini-vials by an
208 automated fraction collector maintained at 4°C (TSE, Uni-
209 ventor, Malta). After collection of the samples, the vials
210 were weighed again to determine sample volumes and
211 stored at -80 °C until off-line analysis. Due to the volume
212 of tubing and microdialysis probes, there was a latency in
213 collecting microdialysate samples of approximately 30 and
214 11 min, in the jugular vein and striatum (ultraslow flow),
215 respectively. Data are therefore shown corrected for this
216 time-lag.

217 At the end of the experiment, the ultraslow flow was
218 turned off, and after a period of 15 min, to allow the pres-
219 sure to dissipate, two more samples were collected and
220 weighed to verify proper functioning of the ultraslow
221 microdialysis dialysis flow through the probe. Samples
222 collected with ultraslow flow turned off should theoretic-
223 ally have less volume and therefore a lower mass. The
224 difference in volume between the samples collected with
225 ultraslow flow and those collected with ultraslow flow
226 turned off indicates the actual rate of the ultraslow flow.
227 This information was used for quality purposes only.

228 The different matrices obtained by the above procedures
229 were analyzed by LC/MS/MS analysis as follows. Samples
230 (5 µL aliquots) were injected onto an HPLC column using
231 an automated sample injector (SIL20-AC-ht, Shimadzu,
232 Japan). Chromatographic separation was performed on a
233 MAX-RP; 3.0 × 100 mm, 2.5 µm column held at 35 °C.
234 The mobile phases consisted of A: 0.1% formic acid (FA)
235 in 2% ACN / 98% UP water and B: 0.1% FA in 90% ACN
236 / 10% UP water at a flow rate of 0.30 mL/min. Mass spec-
237 trometric analyses were performed using an API 5000 MS/
238 MS system consisting of an API 5000 MS/MS detector
239 and a Turbo Ion Spray interface (Applied Biosystems, the
240 Netherlands). The acquisitions were performed in positive
241 ionization mode, with ion spray voltage set at 5.5 kV and
242 a temperature of 600°C. The instrument was operated in
243 multiple-reaction-monitoring mode. Sample concentra-
244 tions were determined by reference to calibration curves
245 fitted using weighted (1/x) regression (csf) or quadratic fit
246 (microdialysate and plasma). Concentrations were calcu-
247 lated with Analyst™ data system (Applied Biosystems,
248 version 1.4.2, the Netherlands).

Fig. 1 Dose & time dependency of NLX-112 levels in plasma, cerebrospinal fluid and striatal extracellular fluid. Symbols are mean \pm SEM of NLX-112 concentration, expressed in ng/mL. Note that the Y axes scales are logarithmic. N=5–6 rats per dose. The right-hand Y-axis in the 'Free striatal ECF' panel shows the concentration of NLX-112 in nM, and the dotted line indicates the in vitro affinity of NLX-112 for the rat 5-HT_{1A} receptor (K_i : 0.85 nM) (Newman-Tancredi et al. 2022). CSF: cerebrospinal fluid; ECF: extracellular fluid



AQ5

249 Recovery indices of NLX-112 from the microdialysis 250 probes

251 In vitro experiments were carried out to establish the per-
252 centage of recovery of NLX-112 across the microdialysis
253 probe membrane. Microdialysis probes were placed in a
254 beaker containing 10^{-8} M of NLX-112 in artificial CSF
255 (same as above) in the presence of bovine serum albumin
256 (BSA, 0.2%) in order to recapitulate the in vivo situation as
257 closely as possible. The beaker contents were continuously
258 stirred and maintained at 37 °C. The probes were perfused
259 in the same manner as in the in vivo experiments, i.e., arti-
260 ficial CSF, but with and without 0.2% BSA. A set of six
261 samples was collected per probe. Microdialysis studies were
262 carried out at a slow flow of 0.8 μ L/min and carrier flow of
263 0.12 μ L/min. In a separate vial 120 μ L of beaker content
264 was diluted with 800 μ L of ultrapurified water, replicating
265 the dilution occurring within the MetaQuant microdialysis
266 probes. In vitro recovery (%) was determined as the ratio
267 between samples, following in vitro microdialysis, and the
268 beaker content concentration.

269 NLX-112 and L-DOPA exposure in plasma and brain 270 following single or combined treatment

271 NLX-112 (0.16 mg/kg i.p.) and L-DOPA (6 mg/kg s.c.) were
272 co-administered with the L-decarboxylase blocker benser-
273 azide (12 mg/kg s.c.). Blood samples were collected at vari-
274 ous time points between 5 min and 4 h after drug adminis-
275 tration (see Fig. 4) via cardiac puncture while the animals
276 were under isoflurane anesthesia, with approximately 0.3 mL

of blood collected at each time point. Following blood col-
lection, brains were removed and homogenized with cold
10 mM PBS (w/v) using a Polytron (3 strokes or more until
homogenous on wet ice, each 30 s), stored at -70 °C until
LC/MS/MS analysis (below). Blood samples were processed
for plasma by centrifugation at approximately 4 °C, 3000 g
within 30 min of collection. Plasma samples were stored in
polypropylene tubes, quickly frozen over dry ice and kept at
-70 °C until LC/MS/MS analysis.

An aliquot of 40 μ L of the plasma sample was protein
precipitated with 160 μ L of the internal standard, the mix-
ture was vortex-mixed well and centrifuged at 4000 rpm
for 20 min, 4 °C. 60 μ L supernatant was then mixed with
120 μ L water/MeOH (v:v, 75:25), vortex-mixed well and
centrifuged at 4 °C. Chromatographic separation of a 5 μ L
sample was performed on an ACQUITY UPLC BEH C18
(2.1 \times 50 mm, 1.7 μ m) column held at 50 °C. The mobile
phases consisted of A: 0.025% formic acid and 1 mM
ammonium ethanoate in water/ACN (v:v, 95:5) and Mobile
Phase B: 0.025% formic acid and 1 mM ammonium nitrate
in acetonitrile/water (v:v, 95:5) at a flow rate of 0.6 mL/
min. Following preparation of the brain samples (above)
and chromatographic separation of a 5 μ L sample, again
using the ACQUITY UPLC BEH C18 (2.1 \times 50 mm, 1.7 μ m)
column held at 50 °C. The mobile phases consisted of A:
0.025% formic acid and 1 mM ammonium acetate in water/
acetonitrile (v:v, 95:5) and B: 0.025% formic acid and 1 mM
ammonium acetate in acetone/water (v:v, 95:5) at a flow rate
of 0.6 mL/min. Diclofenac was used as the internal standard
for the plasma samples and 100 ng/mL labetalol, 100 ng/mL
tolbutamide, and 200 ng/mL diclofenac in acetonitrile for the

308 brain samples. For the analysis of L-DOPA in plasma an ali-
 309 quot of an aliquot of 10 μL sample was protein precipitated
 310 with 200 μL internal standard, the mixture was vortex-mixed
 311 well and centrifuged at 13000 rpm for 15 min, 20–25 $^{\circ}\text{C}$.
 312 200 μL supernatant was removed into another 96-well plate
 313 and evaporated to dry under nitrogen. The dried tube in
 314 96-well plate was then reconstituted with 200 μL water with
 315 0.1% formic acid, vortex-mixed and the plate centrifuged at
 316 4 $^{\circ}\text{C}$. 40 ng/mL acetaminophen and 40 ng/mL nizatidine in
 317 acetonitrile/methanol (v:v, 50:50) with 0.1% formic acid was
 318 used as the internal standard. Chromatographic separation
 319 of a 10 μL sample was performed using an Agilent Eclipse
 320 XDB-C18 4.6 \times 100 mm, 3.5 μm) column at 20 $^{\circ}\text{C}$ with a
 321 flow rate of 0.85 mL/min following injection, with mobile
 322 phase consisting of A: 0.2% formic acid and 0.15% perfluoropropionic
 323 anhydride in water and B: methanol. For the analysis of L-DOPA brain homogenates an aliquot of 60 μL
 324 sample was protein precipitated with 240 μL of the internal
 325 standard, 40 ng/mL acetaminophen and 40 ng/mL and niza-
 326 tidine in acetonitrile/methanol (v:v, 50:50) with 0.1% formic
 327 acid, the mixture was vortex-mixed well and centrifuged at
 328 4000 rpm for 20 min at 4 $^{\circ}\text{C}$. Chromatographic separation
 329 of a 8 μL was performed using an Agilent Eclipse XDB-C18
 330 (4.6 \times 100 mm, 3.5 μm) at 20 $^{\circ}\text{C}$ with a flow rate of 0.85 mL/
 331 min following injection of a 8.0 μL sample, with the mobile
 332 phase consisting of A: 0.2% FA & 0.15% perfluoropropionic
 333 anhydride in water and B: methanol.

335 In all cases mass spectrometric analyses were performed
 336 using API 4000 MS/MS system and concentrations calcu-
 337 lated with reference to calibration a curve.

338 **In vivo occupancy of brain 5-HT_{1A} receptors** 339 **by NLX-112 (microPET imaging)**

340 Male Sprague–Dawley rats (weight 270–480 g, Charles
 341 River, France) were anesthetized with 4% isoflurane, 1 L/
 342 min for 5 min (induction phase), and a catheter (24G, BD
 343 Insyte) was placed into their caudal vein. Anesthesia was
 344 then lowered to 2% isoflurane during the acquisition on
 345 a microPET/CT Inveon (Siemens, Germany), with moni-
 346 toring of the respiratory rate thanks to a pressure sensor
 347 (Biovet, USA). The acquisition started with a CT image
 348 acquisition for 10 min, followed by the i.v. injection of
 349 500 μL of ^{18}F -F13640 (i.e., ^{18}F -NLX-112) at 37 KBq/g
 350 (1 $\mu\text{Ci/g}$) \pm 10%. The radioactivity was measured in a
 351 series of 24 sequential frames of increasing duration from
 352 20 s to 5 min. The total duration of the scan was 60 min.
 353 The images obtained were reconstructed in three dimen-
 354 sions. The regions of interest (ROIs: cingulate cortex, stri-
 355 atum, hippocampus, thalamus, brainstem and cerebellum)
 356 were automatically delineated thanks to an atlas dataset,
 357 after manual positioning of the PET images on an anatomical
 358 MRI template using the Inveon Research Workplace

software (IRW, Siemens). The radioactivity was expressed
 in Bq/cm³ and in SUVs (Standardized Uptake Value) by
 dividing the tissue radioactivity concentration by the
 injected dose of radioactivity per gram of animal. Rats
 underwent four microPET acquisitions with i.p. injection
 of saline or unlabeled NLX-112 at 0.04 mg/kg, 0.16 mg/kg
 or 0.63 mg/kg, 30 min before starting the scan, with a min-
 imal interval of 48 h between two scans. The occupancy
 was estimated using the Lassen plot approach, which is
 required when there is no suitable reference region (as spe-
 cific binding of ^{18}F -F13640 is found in all the rat brain—
 see (Vidal et al. 2018)). For each dose, the differences
 $\text{SUV}_{\text{baseline}} - \text{SUV}_{\text{competition}}$ were calculated for all ROIs and
 plotted as a function of the baseline values, $\text{SUV}_{\text{baseline}}$. A
 linear regression was performed on the respective plots,
 to calculate the receptor occupancy given by the slope
 of the regression line (Cunningham et al. 2010; Takano
 et al. 2014).

377 **Data analysis**

378 PK data were analyzed by non-compartmental approaches
 379 using the PKsolver[®] or Phoenix WinNonlin 6.3.0[®] soft-
 380 ware. The following parameters (units in parenthesis) were
 381 recorded:

- C_{max} : Maximal concentration observed (ng/mL for
 plasma; ng/g for brain)
- T_{max} : Time at which maximal concentration is observed
 (h)
- $T_{1/2}$: Terminal phase half-life (h).
- $\text{AUC}_{0-\text{last}}$: Area under the concentration–time curve
 up to the last measurable concentration (ng.h/mL for
 plasma; ng.h/g for brain)
- $\text{AUC}_{0-\text{last}}$ Ratio: The ratio of the $\text{AUC}_{0-\text{last}}$ from brain
 divided by that of the plasma

392 Data points on graphs show mean \pm SEM values. Rat
 393 cohort size (n) is shown in Figure legends.

394 **In vitro activity at drug transporters**

395 The in vitro activity of NLX-112 as a potential inhibitor or
 396 substrate was investigated at 8 different drug transporters:
 397 P-glycoprotein multidrug transporter (Pgp), Breast Can-
 398 cer Resistance Protein (BCRP), Organo Anion Transport-
 399 ing Polypeptides 1B1 (OATP1B1) and 1B3 (OATP1B3),
 400 Organic Cation Transporter 1 (OCT1) and 2 (OCT2),
 401 Organic Anion Transporter 1 (OAT1) and 3 (OAT3). See
 402 Supplementary Table 1 for details of methodology and
 403 results.

404 **Drugs**

405 NLX-112 (3-Chloro-4-fluorophenyl-[4-fluoro-4-((5-
406 methylpyridin-2-yl)methylamino) methyl]piperidin-
407 1-yl)methanone, fumarate salt), base molecular weight:
408 393.9 g·mol⁻¹, salt molecular weight 509.9 g·mol⁻¹, was
409 synthesized by O2Kem (Castres, France) and administered
410 i.p. in a volume of 2 ml of saline/kg for the total and free
411 plasma, total CSF and free striatum exposure experiment,
412 and 1 ml/kg for the experiment in which NLX-112 and
413 L-DOPA were combined. ¹⁸F-F13640 (i.e., ¹⁸F-NLX-
414 112) radiosynthesis was performed by fluoro-nucleophilic
415 substitution of a nitro-precursor following the method
416 reported in (Vidal et al. 2018), and was administered in
417 a 500 µL saline solution. L-DOPA and benserazide were
418 obtained from commercial sources. Doses refer to the
419 weight of the free base.

420 **Results**421 **Total and free plasma, total CSF and free striatal**
422 **NLX-112 exposure**

423 The in vitro microdialysis probe recovery studies showed
424 that the NLX-112 recovery percentage was higher when
425 Ringer's solution was used without, rather than with, 0.2%
426 BSA (mean ± SEM: 78.2 ± 5.4% versus 43.3 ± 5.8%, respec-
427 tively). BSA was therefore omitted for subsequent in vivo
428 studies.

429 Data from the jugular and femoral vein were similar (data
430 not shown) and were therefore pooled (see Total plasma,
431 Fig. 1 and Table 1). Following i.p. administration, NLX-112
432 total (bound and unbound) plasma concentration was dose-
433 proportional, with C_{max}: 282.6 ng/mL, for 0.63 mg/kg at

15 min; the AUC_{0-last} at this latter dose was 360.0 ng·h/mL.
T_{1/2} was inversely proportional to the dose administered, and
calculated as 0.87 h for 0.63 mg/kg.

Peak free (unbound) plasma concentrations were
60–70 times lower than those for total plasma and were
observed at with T_{max} values four times longer (1 h ver-
sus 15 min, for free plasma and total plasma, respec-
tively) for 0.16 and 0.63 mg/kg. The AUC_{0-last} values
were 33–38 times lower than those calculated for total
plasma; T_{1/2} values were roughly twice as long as the
total plasma ones.

Concerning the concentrations in the CSF, C_{max} val-
ues were about 3 to 4 times higher than those for free
plasma at 0.16 and 0.63 mg/kg and observed at earlier
time-points; AUC_{0-last} values were also notably higher
by a factor of 2–3. Note that the T_{1/2} at the lowest dose
departed from what would be expected. Lastly, in a brain
structure (striatum) involved in motor control, C_{max} for
NLX-112 was about half that for total CSF, and quite
close to the free plasma concentrations. T_{max} values were
equivalent to those for total CSF at the two higher doses;
AUC_{0-last} values were similar to those observed for free
plasma.

Quantitative analysis of the AUCs of concentrations
of NLX-112 in all four tissues revealed that there was
a highly linear and significant (all F(1,1) > 192.4, all
p < 0.01) relationship between the dose of NLX-112 and
its exposure level (supplementary Fig. 1).

462 **In vivo occupancy of brain 5-HT_{1A} receptors**
463 **by NLX-112 (microPET imaging)**

464 Intravenous injection of ¹⁸F-F13640 (i.e., ¹⁸F-NLX-112)
465 produced a distinctive pattern of binding to brain 5-HT_{1A}
466 receptors (see images of a representative rat, Fig. 2, panel
467 A), with regions in red (corresponding to highest uptake)

Table 1 Pharmacokinetic parameters of NLX-112 in rat brain and plasma

AQ6

NLX-112 dose (mg/kg, i.p.)	Total plasma			Free plasma			Total CSF			Free striatal ECF		
	0.04	0.16	0.63	0.04	0.16	0.63	0.04	0.16	0.63	0.04	0.16	0.63
C _{max}	7.6	44.9	282.6	0.13	0.76	4.0	0.31	2.4	18.7	0.15	1.1	3.9
T _{max}	0.5	0.25	0.25	0.5	1	1	0.5	0.25	0.25	1.75	1.25	1.25
T _{1/2}	1.63	0.91	0.87	3.09	1.96	1.88	13.18	1.11	0.91	1.42	1.40	0.95
AUC _{0-last}	11.5	75.1	360.0	0.3	2.0	10.9	0.8	3.8	24.9	0.4	2.5	8.0

NLX-112 levels were measured in plasma (total and free), in cerebrospinal fluid (CSF) and in striatal extracellular fluid (ECF)

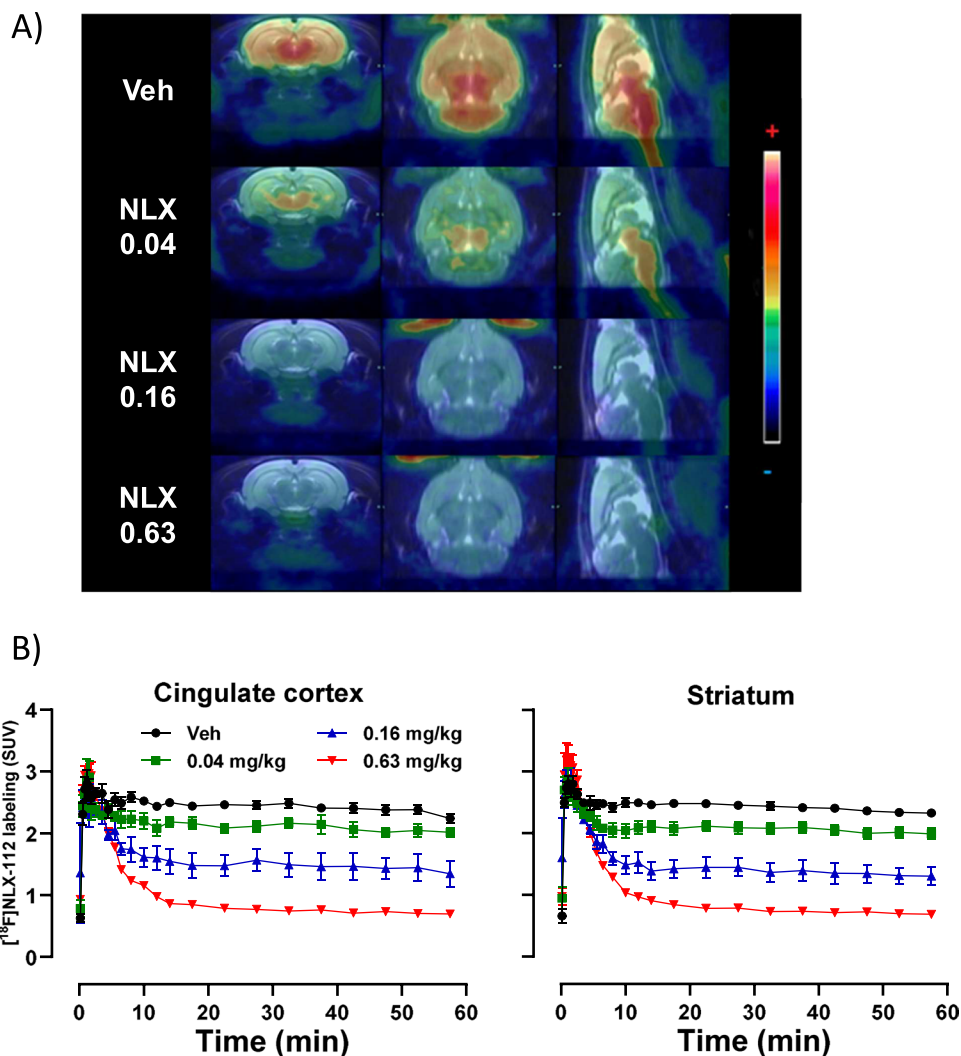
C_{max}: Maximal concentration observed (ng/mL for plasma; ng/g for brain)

T_{max}: Time at which maximal concentration is observed (h)

T_{1/2}: Terminal phase half-life. The time it takes for the concentration levels to fall by 50% of their value (h)

AUC_{0-last}: Area under the concentration–time curve up to the last measurable concentration (ng·h/mL for plasma; ng·h/g for brain)

Fig. 2 Occupancy of rat brain 5-HT_{1A} receptors by NLX-112. Panel **A**: Coronal, transverse and sagittal representative summed microPET images on corresponding MRI rat brain template, showing ¹⁸F-F13640 (i.e., ¹⁸F-NLX-112) labeling in rat brain after pre-injection of vehicle (saline) or increasing doses of unlabeled NLX-112 (same scale used for all images). Panel **B**: Time course of the Standardized Uptake Values (SUVs) following administration of vehicle or NLX-112 (0.04, 0.16 or 0.63 mg/kg i.p.). Symbols are the mean ± SEM. Saline or NLX-112 were injected i.p. 30 min prior to the start of the microPET image acquisition (immediately before i.v. injection of ¹⁸F-F13640). N = 3–4 rats per treatment



468 localized mainly in the brainstem, thalamus and cortex.
 469 Treatment with unlabeled NLX-112, 30 min i.p. before
 470 the i.v. injection of ¹⁸F-F13640, dose-dependently reduced
 471 ¹⁸F-F13640 binding, as illustrated by a shift towards
 472 the blue color (corresponding to lowest uptake) in all
 473 brain regions examined. In other words, NLX-112 com-
 474 peted with ¹⁸F-F13640 for binding to the target 5-HT_{1A}
 475 receptors.

476 Quantitative analysis of the competition between ¹⁸F-
 477 F13640 and unlabeled NLX-112 in the striatum and cin-
 478 gulate cortex confirmed that NLX-112 produced a robust
 479 dose-dependent reduction of the radiotracer uptake, that
 480 was readily observed after the initial peak 10 min after the
 481 start of microPET image acquisition, time at which the radi-
 482 otracer uptake reached a plateau (Fig. 2, panel B). When
 483 averaging the last six frames of acquisition for the striatum
 484 and the cingulate cortex, the reduction was 14% and 13%
 485 at 0.04 mg/kg, 43% and 40% at 0.16 mg/kg and 70% and
 486 70% at 0.63 mg/kg, respectively. Similar data were observed
 487 for 2 other brain regions examined (hippocampus and brain

stem; data not shown). The analysis of occupancy of 5-HT_{1A}
 receptors by unlabeled NLX-112, as estimated by the Lassen
 plot approach using the SUV uptake values in the different
 ROIs, yielded occupancy values of 11%, 64% and 93% at
 doses of 0.04, 0.16 and 0.63 mg/kg, respectively.

Relationship between the in vivo occupancy of 5-HT_{1A} receptors by NLX-112 and its anti-dyskinetic activity

Previous studies showed that NLX-112 dose-dependently
 reduced abnormal involuntary movements (AIMs, a rodent
 analog of LID) in hemi-parkinsonian rats with a unilateral
 6-OHDA lesion of the striatum and chronically treated
 with L-DOPA to produce LID (Iderberg et al. 2015). Here
 we show that there is a relationship between increased
 in vivo occupancy of central 5-HT_{1A} receptors by NLX-
 112 (present microPET imaging data), and its efficacy to
 decrease AIMs (behavioral data extracted from Fig. 3 in
 Iderberg et al. 2015). Hence, in rats treated with vehicle,

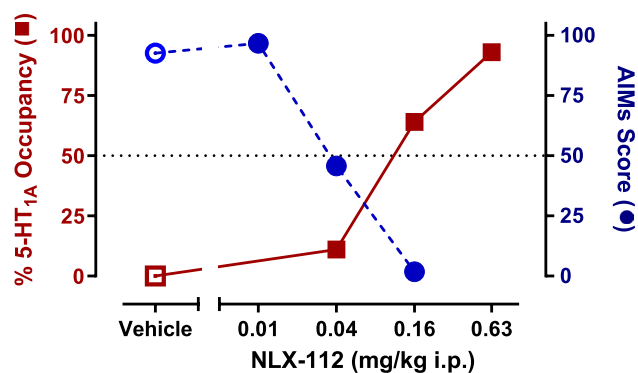
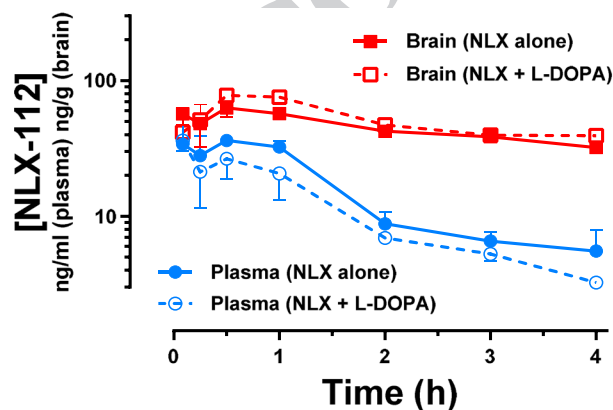


Fig. 3 Anti-dyskinetic activity of NLX-112 correlated to its occupancy of rat striatal 5-HT_{1A} receptors. Symbols are the mean. Data for striatal 5-HT_{1A} receptors occupancy are from the ¹⁸F-NLX-112 microPET imaging experiment described herein. Data for the anti-dyskinetic activity of NLX-112 are adapted from (Iderberg et al. 2015) using the AIMS (Abnormal involuntary movements) scale for observation of rat behavior over a 3 h period. The dose of 0.63 mg/kg i.p. was not tested for anti-AIMS activity. The ED₅₀ for reduction of AIMS is approximately 0.04 mg/kg, corresponding to a total plasma exposure of 11.5 ng.h/ml (see AUC data in Table 1). The ED₅₀ for receptor occupancy is approximately 0.1 mg/kg, corresponding to a total plasma exposure of about 50 ng.h/ml

L-DOPA (6 mg/kg s.c.) elicits a high AIMS score (92.6), which is dose-dependently decreased as the occupancy of 5-HT_{1A} receptors by NLX-112 increases. At the dose of 0.16 mg/kg i.p., at which there is a near total disappearance of AIMS (score reduced from 92.6 to 1.8), the occupancy of 5-HT_{1A} receptors was 64%. A robust anti-LID activity (approximate halving of AIMS score) can be observed with a moderate (11%) level of occupancy of 5-HT_{1A} receptors elicited by NLX-112 at 0.04 mg/kg i.p..



Absence of pharmacokinetic interaction between NLX-112 & L-DOPA

Co-administration of NLX-112 (0.16 mg/kg i.p.) with L-DOPA (6 mg/kg s.c.; together with benserazide, 12 mg/kg s.c.) had no discernible influence on the plasma and brain concentrations of either NLX-112 or L-DOPA alone. Concentration versus time curves for NLX-112 and L-DOPA, whether for NLX-112 or L-DOPA administered alone, or for their combined administration (L-DOPA + NLX-112), were quasi superimposable, both for plasma and brain (Fig. 4). Examination of calculated PK parameters confirms this lack of interaction, for all four parameters examined: C_{max}, T_{max}, T_{1/2}, AUC_{0-last} and AUC_{0-last} Ratio (the ratio of the AUC_{0-last} from the brain divided by that of the plasma) for compounds alone, or when combined (Table 2). As a reminder, this experiment was done to verify that the reduction of AIMS by NLX-112 in the rat LID model is not associated with changes in brain levels of L-DOPA.

NLX-112 is neither an inhibitor nor a substrate at 8 drug transporters

NLX-112 was very weakly active as an inhibitor of 8 transporters (PgP, BCRP, OATP1B1, OATP1B3, OCT1, OCT2, OAT1, OAT3), including some that are located on the blood-brain barrier (BBB). IC₅₀ values ranged from 9.8 μM to over 100 μM (Supplementary Table 1). As a reminder, at doses active in rat motor disorders models (0.04 to 0.63 mg/kg i.p.), the corresponding free plasma C_{max} of NLX-112 is in the range of 0.3 to 10.2 ng/ml, i.e., concentrations of 0.75 to 25.5 nM. These therapeutically relevant concentrations are therefore at least 1000-fold lower than the IC₅₀ values listed above. NLX-112, tested as a substrate, also showed

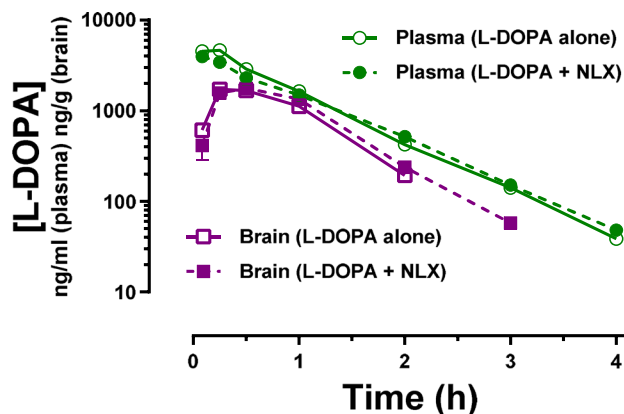


Fig. 4 Absence of pharmacokinetic interaction between NLX-112 and L-DOPA. Symbols are the mean and SEM of drug concentrations, expressed in ng/ml (for plasma) or ng/g (for brain). Note that the X axes scales are logarithmic. L-DOPA (6 mg/kg s.c.) was co-

administered with the L-decarboxylase blocker benserazide (12 mg/kg s.c.); NLX-112 was administered at 0.16 mg/kg i.p.. N=3 rats per point

Table 2 PK parameters of NLX-112 and L-DOPA administered alone or in combination

	NLX-112				L-DOPA			
	NLX-112 Alone		With L-DOPA		L-DOPA Alone		With NLX-112	
	Plasma	Brain	Plasma	Brain	Plasma	Brain	Plasma	Brain
C_{max}	36.3	63.1	36.2	78.1	4640	1715	3967	1763
T_{max}	0.0833	0.50	0.50	0.50	0.25	0.25	0.0833	0.50
$T_{1/2}$	1.13	3.61	1.17	3.11	0.56	0.47	0.59	0.44
AUC_{0-last}	48.3	180.6	66.2	208.2	4423	1998	3875	2310
Brain:Plasma Ratio	3.74		3.15		0.45		0.60	

NLX-112 was administered i.p. at 0.16 mg/kg; L-DOPA was administered s.c. at 6 mg/kg, with 12 mg/kg s.c. benserazide

C_{max} : Maximal concentration observed (ng/mL for plasma; ng/g for brain)

T_{max} : Time at which maximal concentration is observed (h)

$T_{1/2}$: Terminal phase half-life (time for the concentration levels to fall by 50% of their value, in h)

AUC_{0-last} : Area under the concentration–time curve up to the last measurable concentration (ng.h/mL for plasma; ng.h/g for brain)

Brain:Plasma Ratio: Based on the AUC_{0-last} from the brain divided by that of the plasma

545 essentially negligible interaction with these 8 transporters,
546 (Supplementary Table 2. Although the maximal concentration
547 tested for the first two transporters was 2 μ M (as opposed to
548 100 μ M for the others), the results indicate that there is at
549 least a 100-fold separation versus therapeutically relevant
550 concentrations of NLX-112 (see above). It is therefore very
551 unlikely that NLX-112 will block or act as a substrate for
552 these drug transporters, at least as concerns those present at
553 the level of the BBB. **INSERT SECTION HEAD HERE**

554 The present study of NLX-112, combining pharmacodynamic,
555 pharmacokinetic and brain imaging data in rats,
556 shows that, following acute systemic administration: 1)
557 NLX-112 exposure in plasma and brain peaks rapidly and is
558 observed for an extended period of time; 2) NLX-112 occupies
559 brain 5-HT_{1A} receptors at pharmacologically-relevant
560 doses; 3) a moderate level of brain 5-HT_{1A} receptors occupancy
561 is sufficient to efficaciously reduce the AIMS score
562 (a rat readout of LID) and 4) NLX-112 does not modify the
563 plasma and brain pharmacokinetic profile of L-DOPA (and
564 vice-versa).

565 NLX-112 plasma and brain exposure 566 at pharmacological doses

567 The present study shows that NLX-112 rapidly penetrates
568 the brain following systemic administration and that it has
569 an extended half-life therein. Thus, at a dose of 0.63 mg/
570 kg i.p., total plasma NLX-112 reached a C_{max} of 282.6 ng/
571 mL within 15 min, with levels dropping by about 90% at
572 3 h. This is similar to values obtained in a previous rat
573 PK study (Bardin et al. 2005) where, at the same dose of
574 0.63 mg/kg i.p., total plasma C_{max} was 293.4 ng/mL with
575 a T_{max} of 15 min, and a decrease of about 90% at 4 h. It is
576 notable that the rapid absorption to plasma of NLX-112

577 is also seen in higher species: in marmosets, total plasma
578 C_{max} at a dose of 0.4 mg/kg p.o. at 1 h was 254.6 ng/ml
579 and decreased by around 80% at 4 h (Fisher et al. 2020).
580 In macaques, total plasma C_{max} of NLX-112 at a dose of
581 0.1 mg/kg p.o. was 50.6 ng/mL at 30 min, with levels
582 dropping by around 90% at 4 h (Depoortere et al. 2020).
583 The PK parameters of NLX-112 have also been explored
584 in humans: a single 1 mg oral dose of NLX-112 as an
585 immediate-release tablet produced a total plasma C_{max} of
586 22 ng/mL at a T_{max} of 2 h (Paillard et al. 2016). Overall,
587 the data from all the species indicate consistently rapid
588 absorption properties of NLX-112 with substantial exposure
589 in blood plasma.

590 In addition to rapid absorption in plasma, the present
591 data also point to rapid and robust brain penetration at
592 levels that are sufficient to bind to 5-HT_{1A} receptors. This
593 conclusion is supported by the free striatal ECF levels
594 of NLX-112 at a pharmacologically meaningful dose of
595 0.16 mg/kg (range: 0.4–1.1 ng/mL, i.e. 1.0 to 2.8 nM).
596 These are slightly above the binding affinity of NLX-112
597 for the rat 5-HT_{1A} receptor ($K_i = 0.85$ nM) (Newman-
598 Tancredi et al. 2017), suggesting that, when NLX-112 is
599 administered at that dose, it produces free brain concentrations
600 that are sufficient to bind and activate 5-HT_{1A} receptors
601 and thereby elicit complete suppression of AIMS in
602 the rat model of LID (Iderberg et al. 2015). It should be
603 noted that the brain concentrations measured here for striatum
604 (3.9 ng/mL at a dose of 0.63 mg/kg i.p.) are similar
605 to those reported previously for rat hippocampus (3.6 ng/
606 mL also at 0.63 mg/kg i.p.), using similar analyses from
607 hippocampal microdialysate samples (Bardin et al. 2005).
608 Moreover the two studies found similar T_{max} values of 1 h
609 for the hippocampus (Bardin et al. 2005), and 75 min
610 herein for the striatum. This suggests that NLX-112

611 distributes uniformly in brain and is able to engage its
612 molecular target (i.e., 5-HT_{1A} receptors) in different brain
613 regions (see further comments below).

614 Relationship between brain 5-HT_{1A} receptor 615 occupancy and anti-dyskinetic activity in rats

616 The availability of ¹⁸F-F13640 (i.e., ¹⁸F-NLX-112), a
617 radiolabeled form of NLX-112, enables direct measure-
618 ment of its distribution in rat brain by PET imaging, as
619 also previously done in cats and NHP (Vidal et al. 2018)
620 and in humans (Colom et al. 2020; Courault et al. 2023).
621 This allows investigation of the occupancy of function-
622 ally active population of 5-HT_{1A} receptors. This is a criti-
623 cal point because previous PET studies using classical
624 antagonist radiotracers of 5-HT_{1A} receptors failed to detect
625 significant occupancy by 5-HT_{1A} agonists at pharmaco-
626 logically active doses, a finding which is likely due to the
627 presence of only a low proportion of active state receptors
628 out of the total receptor population (Bantick et al. 2004).
629 Previous work with ¹⁸F-NLX-112 showed that it very rap-
630 idly penetrates the brain and specifically labels 5-HT_{1A}
631 receptors with an extended half-life in rat, cat, macaque
632 and human subjects (Vidal et al. 2018) (Colom et al. 2020;
633 Courault et al. 2023).

634 Here, unlabeled NLX-112 dose-dependently inhibited
635 ¹⁸F-F13640 binding, with near-maximal occupancy being
636 observed at 0.63 mg/kg. This profile was essentially iden-
637 tical across all brain regions examined, providing further
638 evidence that NLX-112 can interact with 5-HT_{1A} recep-
639 tors in different brain regions with the same dose–response
640 relationship. Importantly, as well as demonstrating tar-
641 get engagement, these data enable estimation of central
642 occupancy of functional 5-HT_{1A} receptors necessary for
643 therapeutic-like effects. Thus, even a modest occupancy
644 of active-state 5-HT_{1A} receptors was sufficient to elicit
645 robust antidyskinetic activity. Indeed, the NLX-112 dose of
646 0.04 mg/kg i.p., which has been previously shown to dimin-
647 ish AIMs by about half (Iderberg et al. 2015), produced
648 occupancy of only 11%, whereas the dose of 0.16 mg/kg
649 i.p. occupied 60–70% of active-state 5-HT_{1A} receptors in
650 brain, and thereby elicited complete suppression of AIMs in
651 the rat model of LID. This suggests that active-state 5-HT_{1A}
652 receptors are highly sensitive to agonist stimulation, at least
653 in the case of a full agonist such as NLX-112. It should be
654 noted, however, that changes in 5-HT_{1A} receptor expres-
655 sion and sensitivity occur upon lesioning of dopaminergic
656 neurons and upon repeated L-DOPA administration (Chaib
657 et al. 2023; Vidal et al. 2021), so these findings would ben-
658 efit from further investigation using ‘hemi-parkinsonian’
659 rats (i.e., with unilateral 6-OHDA lesions of the Substantia
660 nigra, a rodent model of LID).

Absence of PK interaction between NLX-112 and L-DOPA

661 The presence of NLX-112 did not influence the levels of
662 L-DOPA, whether in the plasma or in the whole brain. This
663 is important because the reduction of AIMs in hemi-parkin-
664 sonian rats by NLX-112 could be hypothesized to be con-
665 secutive to a reduction in available L-DOPA. The absence
666 of a pharmacokinetic interaction, both peripherally and
667 centrally, therefore supports the conclusion that the potent
668 and efficacious anti-LID activity of NLX-112 stems from a
669 genuine pharmacodynamic phenomenon, mediated by NLX-
670 112's activation of central 5-HT_{1A} receptors (rather than by
671 a decrease in levels of L-DOPA). This is consistent with the
672 observation that the anti-LID effects of NLX-112 are abol-
673 ished by a selective 5-HT_{1A} receptor antagonist, WAY100,635
674 (Iderberg et al. 2015), indicating specific target interaction.
675
676

Limitations of the study

677 Some limitations of the present study should be noted.
678 Firstly, the PK profile of NLX-112 was investigated in male
679 rats and might differ in female rats. However, a pilot PK
680 study in female Sprague–Dawley rats showed that, at a NLX-
681 112 dose of 0.63 mg/kg i.p., total plasma C_{max} was 301 ng/
682 mL with T_{max} at 30 min (Neurolix unpublished data) which
683 is similar to values reported in Table 1 for males of the same
684 strain (C_{max} 282.6 ng/mL, T_{max} 15 min), suggesting that
685 there is no sex difference in PK parameters. Secondly, the
686 present study tested only acute administration of NLX-112
687 and it would be valuable to conduct PK studies following
688 a protracted treatment (e.g., 2–3 weeks) with NLX-112, to
689 determine whether there is drug accumulation in particular
690 brain regions. Lastly, the present studies were conducted in
691 ‘normal’ rats, and it would be informative to conduct experi-
692 ments in hemi-parkinsonian rats that have been subjected
693 to a protracted treatment with L-DOPA to produce LID, as
694 mentioned above.
695

Conclusions and perspectives

696 To summarize, NLX-112 presents a PK profile in rats
697 highly compatible with that of drugs developed for phar-
698 macotherapeutic treatment of CNS diseases. Indeed, fol-
699 lowing acute i.p. treatment at pharmacologically relevant
700 doses, NLX-112 rapidly penetrates its target tissue (the
701 brain), where it remains detectable for several hours and
702 with a high target engagement of central 5-HT_{1A} recep-
703 tors, as assessed by microPET brain imaging. Further-
704 more, based on total exposure (Table 2) its brain:plasma
705 AUC ratio is high (almost 4), a favorable property for a
706 drug under development for treatment of CNS disorders
707 (although the ratio between free striatal and free plasma
708

709 concentrations, i.e. K_p , u_u values, have not been assessed).
 710 Lastly, there is no detectable PK interaction between
 711 NLX-112 and L-DOPA, whether in brain or plasma,
 712 indicating that the two compounds can be assessed inde-
 713 pendently for dosing purposes. These findings support
 714 the further development of NLX-112 for the treatment of
 715 LID, notably following the recent positive phase 2a clinical
 716 trial in PD patients, which met both its primary out-
 717 come of safety and tolerability, and secondary outcomes
 718 of efficacy against both LID and parkinsonian motor dis-
 719 ability (Svenningsson et al. 2023). Nevertheless, further
 720 PK and 5-HT_{1A} receptor occupancy studies in human sub-
 721 jects would be useful to establish the extent to which the
 722 present observations in rat translate to a clinical context.

723 **Supplementary Information** The online version contains supplement-
 724 ary material available at <https://doi.org/10.1007/s00210-024-03323-0>.

725 **Authors contribution** All authors have approved the final version of the
 726 manuscript and declare that all data were generated in-house and that no
 727 paper mill was used. Ronan Depoortere: Data interpretation; Writing:
 728 original draft, review & editing. Andrew C. McCreary: Conceptualiza-
 729 tion, Data curation, Formal analysis, Visualization, Writing: review &
 730 editing. Benjamin Vidal: Conceptualization, Data curation, Formal analy-
 731 sis, Visualization, Writing: review & editing. Luc Zimmer: Conceptual-
 732 ization, Data curation, Formal analysis, Visualization, Writing: review &
 733 editing. Mark Varney: Conceptualization, Data interpretation, Visualiza-
 734 tion, Writing: review & editing. Adrian Newman-Tancredi: Conceptual-
 735 ization, Data interpretation, Visualization, Writing: review & editing.

736 **Funding** Financial support for pharmacokinetic studies was received
 737 from the Michael J. Fox Foundation for Parkinson's Research (grant
 738 ID# 9233). The microPET study was supported by the LABEX
 739 PRIMES (ANR-11-LABX-0063) of Université de Lyon and the
 740 'Investissements d'Avenir' program (ANR-11-IDEX-0007) from the
 741 French National Research Agency (ANR) and the imaging platform,
 742 CERMEP (Lyon, France).

743 **Data availability** Data supporting the findings of this study are avail-
 744 able within the paper and its Supplementary Information.

745 Declarations

746 **Ethical approval** ANT, MAV and RYD are shareholders and/or
 747 employees of Neurolixis. The other authors declare no competing
 748 interests.

749 References

750 Bantick RA, Rabiner EA, Hirani E et al (2004) Occupancy of agonist
 751 drugs at the 5-HT_{1A} receptor. *Neuropsychopharmacology* : Offi-
 752 cial Publication of the American College of Neuropsychophar-
 753 macology 29(5):847–859
 754 Bardin L, Assie MB, Pelissou M et al (2005) Dual, hyperalgesic,
 755 and analgesic effects of the high-efficacy 5-hydroxytryptamine
 756 1A (5-HT_{1A}) agonist F 13640 [(3-chloro-4-fluoro-phenyl)-
 757 [4-fluoro-4-[(5-methyl-pyridin-2-ylmethyl)-amino]-me thyl]
 758 piperidin-1-yl]methanone, fumaric acid salt]: relationship with

5-HT_{1A} receptor occupancy and kinetic parameters. *J Pharma-
 col Exp Ther* 312(3):1034–1042
 Barnes NM, Ahern GP, Becamel C et al (2021) International Union
 of Basic and Clinical Pharmacology. CX. Classification of
 Receptors for 5-hydroxytryptamine; Pharmacology and Func-
 tion. *Pharmacol Rev* 73(1):310–520
 Borroto-Escuela DO, Ambrogini P, Chruscicka B et al (2021) The
 Role of Central Serotonin Neurons and 5-HT Heteroreceptor
 Complexes in the Pathophysiology of Depression: A Historical
 Perspective and Future Prospects. *Int J Mol Sci* 22(4):1927
 Caccia S, Muglia M, Mancinelli A et al (1983) Disposition and
 metabolism of buspirone and its metabolite 1-(2-pyrimidinyl)-
 piperazine in the rat. *Xenobiotica* 13(3):147–153
 Celada P, Bortolozzi A, Artigas F (2013) Serotonin 5-HT_{1A} recep-
 tors as targets for agents to treat psychiatric disorders: rationale
 and current status of research. *CNS Drugs* 27(9):703–716
 Chaib S, Vidal B, Bouillot C et al (2023) Multimodal imaging study
 of the 5-HT(1A) receptor biased agonist, NLX-112, in a model
 of L-DOPA-induced dyskinesia. *Neuroimage Clin* 39:103497
 Colom M, Costes N, Redoute J et al (2020) [18F]-F13640 PET imaging
 of functional receptors in humans. *Eur J Nucl Med Mol Imaging*
 47(1):220–221
 Colom M, Vidal B, Fieux S et al (2021) [(18)F]F13640, a 5-HT_{1A}
 Receptor Radiopharmaceutical Sensitive to Brain Serotonin Fluc-
 tuations. *Front Neurosci* 15:622423
 Courault P, Lancelot S, Costes N et al (2023) [(18)F]F13640: a selec-
 tive agonist PET radiopharmaceutical for imaging functional
 5-HT(1A) receptors in humans. *Eur J Nucl Med Mol Imaging*
 50(6):1651–1664
 Cunningham VJ, Rabiner EA, Slifstein M et al (2010) Measuring drug
 occupancy in the absence of a reference region: the Lassen plot
 re-visited. *J Cereb Blood Flow Metab* 30(1):46–50
 Depoortere R, Johnston TH, Fox SH et al (2020) The selective 5-HT_{1A}
 receptor agonist, NLX-112, exerts anti-dyskinetic effects in MPTP-
 treated macaques. *Parkinsonism Relat Disord* 78:151–157
 Fisher R, Hikima A, Morris R et al (2020) The selective 5-HT_{1A} recep-
 tor agonist, NLX-112, exerts anti-dyskinetic and anti-parkinsonian-
 like effects in MPTP-treated marmosets. *Neuropharmacology*
 167:107997
 Iderberg H, McCreary AC, Varney MA et al (2015) NLX-112, a novel
 5-HT_{1A} receptor agonist for the treatment of L-DOPA-induced
 dyskinesia: Behavioral and neurochemical profile in rat. *Exp Neurol*
 271:335–350
 Levigoureux E, Vidal B, Fieux S et al (2019) Serotonin 5-HT_{1A} recep-
 tor biased agonists induce different cerebral metabolic responses:
 A [18F]FDG PET study in conscious and anesthetized rats. *ACS
 Chem Neurosci* 10(7):3108–3119
 Newman-Tancredi A, Martel JC, Cosi C et al (2017) Distinctive
 in vitro signal transduction profile of NLX-112, a potent and effi-
 cacious serotonin 5-HT_{1A} receptor agonist. *J Pharm Pharmacol*
 69(9):1178–1190
 Newman-Tancredi A, Depoortere RY, Kleven MS et al (2022) Trans-
 lating biased agonists from molecules to medications: Serotonin
 5-HT_{1A} receptor functional selectivity for CNS disorders. *Phar-
 macol Ther* 229:107937
 Pagano G, Niccolini F, Politis M (2017) The serotonergic system
 in Parkinson's patients with dyskinesia: evidence from imag-
 ing studies. *J Neural Transm (vienna)*. <https://doi.org/10.1007/s00702-017-1823-7>
 Paillard B, Del Frari L, Brunner V, et al. (2016) A method for treating
 movement disorders with befiradol. In: WO2016/005527A1 (ed).
 Paxinos G, Watson C (2007) *The Rat Brain in Stereotaxic Coordinates*.
 Academic Press
 Pourhamzeh M, Moravej FG, Arabi M, et al (2021) The Roles of
 Serotonin in Neuropsychiatric Disorders. *Cell Mol Neurobiol*.

824	Epub ahead of print 2021/03/03. https://doi.org/10.1007/s10571-021-01064-9		
825	Prinssen EP, Colpaert FC, Koek W (2002) 5-HT1A receptor activation and anti-cataleptic effects: high-efficacy agonists maximally inhibit haloperidol-induced catalepsy. <i>Eur J Pharmacol</i> 453(2–3):217–221		
826		Vidal B, Fieux S, Colom M et al (2018) [18F]-F13640 preclinical evaluation in rodent, cat and primate as a 5-HT1A receptor agonist for PET neuroimaging. <i>Brain Struct Funct</i> 223(6):2973–2988	843
827			844
828		Vidal B, Bolbos R, Redoute J et al (2020) Pharmacological MRI to investigate the functional selectivity of 5-HT1A receptor biased agonists. <i>Neuropharmacology</i> 172:107867	845
829			846
830	Svenningsson P, Odin P, Bergquist F, et al (2023) NLX-112 has favorable safety, tolerability and efficacy against levodopa-induced dyskinesia (LID) in a randomized, double-blind, placebo-controlled, proof-of-concept Ph2A study. In: World Parkinson's Congress, July 4–7, 2023, Barcelona, Poster Board #LBP38.31		847
831		Vidal B, Levigoureux E, Chaib S et al (2021) Different alterations of agonist and antagonist binding to 5-HT1A receptor in a rat model of Parkinson's disease and levodopa-induced dyskinesia : a microPET study. <i>Journal of Parkinson Disease</i> 11(3):1257–1269	848
832			849
833			850
834			851
835			852
836	Takano A, Gulyas B, Varnas K et al (2014) Low brain CB1 receptor occupancy by a second generation CB1 receptor antagonist TM38837 in comparison with rimonabant in nonhuman primates: a PET study. <i>Synapse</i> 68(3):89–97	Publisher's Note Springer Nature remains neutral with regard to jurisdictional claims in published maps and institutional affiliations.	853
837			854
838		Springer Nature or its licensor (e.g. a society or other partner) holds exclusive rights to this article under a publishing agreement with the author(s) or other rightsholder(s); author self-archiving of the accepted manuscript version of this article is solely governed by the terms of such publishing agreement and applicable law.	855
839			856
840	Vidal B, Fieux S, Billard T et al (2014) Radiopharmacological evaluation of [18F]F13640, a novel 5-HT1A receptor agonist. <i>J Nuclear Medicine</i> 55(Supp. 1):1100		857
841			858
842			859

Journal:	210
Article:	3323

Author Query Form

Please ensure you fill out your response to the queries raised below and return this form along with your corrections

Dear Author

During the process of typesetting your article, the following queries have arisen. Please check your typeset proof carefully against the queries listed below and mark the necessary changes either directly on the proof/online grid or in the 'Author's response' area provided below

Query	Details Required	Author's Response
AQ1	Please check if the article title was captured and presented correctly.	
AQ2	Please confirm if the authors names are presented accurately and in the correct sequence (extended given name, middle name/initial, family name). Also kindly confirm the details in the metadata are correct.	
AQ3	Please check the provided affiliation if captured and presented correctly.	
AQ4	Please check and confirm if section heads and subheads are assigned to appropriate levels. Otherwise, kindly amend.	
AQ5	Please check if all figure captions are captured and presented correctly.	
AQ6	Please check if the table captions, cell entries, and footnotes are captured and presented correctly.	
AQ7	According to our submission guidelines for authors, first subsection "Important Submission Policy" (https://www.springer.com/journal/210/submissionguidelines#Instructions%20for%20Authors_Important%20Submission%20Policy), ALL papers must include the following statement in the section "Authors Contributions": The authors declare that all data were generated in-house and that no paper mill was used. This is not the case in your accepted article. Please confirm that we can add this sentence in the section "Authors Contributions".	
AQ8	Please check if back matter sections are captured/presented correctly. Otherwise, kindly amend.	
AQ9	Please check supplementary materials and information if captured and presented correctly.	
AQ10	Please verify reference Borroto-Escuela et al., 2021 if captured and presented correctly.	